A Leakage-based Method for Mitigation of Faulty Reconfigurable Intelligent Surfaces

Nairy Moghadas Gholian*, *Student Member, IEEE,* Marco Rossanese†, *Student Member, IEEE,* Placido Mursia†, *Member, IEEE,* Andres Garcia-Saavedra†, *Member, IEEE,*, Arash Asadi*, *Senior Member, IEEE*, Vincenzo Sciancalepore†, *Senior Member, IEEE*, and Xavier Costa-Pérez†, *Senior Member, IEEE*
*Technical University of Darmstadt (TUDa), Darmstadt, Germany
ngholian@wise.tu-darmstadt.de, aasadi@wise.tu-darmstadt.de
†NEC Laboratories Europe GmbH, Heidelberg, Germany
{name.surname}@neclab.eu

GLOBECOM 2023 - 2023 IEEE Global Communications Conference | 979-8-3503-1090-0/23/$31.00 ©2023 IEEE | DOI: 10.1109/GLOBECOM54140.2023.10437177

***Abstract*—Reconfigurable Intelligent Surfaces (RISs) are expected to be massively deployed in future beyond-5th generation wireless networks, thanks to their ability to programmatically alter the propagation environment, inherent low-cost and low-maintenance nature. Indeed, they are envisioned to be implemented on the facades of buildings or on moving objects. However, such an innovative characteristic may potentially turn into an involuntary negative behavior that needs to be addressed: an undesired signal scattering. In particular, RIS elements may be prone to experience failures due to lack of proper maintenance or external environmental factors. While the resulting Signal-to-Noise-Ratio (SNR) at the intended User Equipment (UE) may not be significantly degraded, we demonstrate the potential risks in terms of unwanted spreading of the transmit signal to non-intended UEs. In this regard, we consider the problem of mitigating such undesired effectby proposing two simple yet effective algorithms, which are based on maximizing the Signal-to-Leakage-and-Noise-Ratio (SLNR) over a predefined two-dimensional (2D) area and are applicable in the case of perfect channel-state-information (CSI) and partial CSI, respectively. Numerical and full-wave simulations demonstrate the added gains compared to leakage-unaware and reference schemes.**

***Index Terms*—Reconfigurable Intelligent Surfaces, mmWave, optimization, faulty antennas.**

I. Introduction

The proliferation of Reconfigurable Intelligent Surface (RIS)-assisted wireless networks has sparked a surge of research into the design and optimization of these systems, focusing on achieving congruent goals of improved spectral efficiency, enhanced coverage, and reduced energy consumption. Indeed, the RIS technology is considered the enabler of the *Smart Radio Environment* for future wireless networks [1], owing to its ability to manipulate the signal from the transmitter to the receiver [2]. In this regard, extensive efforts have been devoted towards demonstrating the feasibility of these surfaces through proof-of-concepts [3], and realistic modelling [4].

However, similarly to any other piece of hardware, RISs can fail. This may be due to a variety of causes, including aging, external phenomena (installation on moving objects [5]), environmental factors, or disaster situations [6]. Moreover, due to the large number of elements in RISs, the maintenance and replacement of faulty RISs may be difficult and costly to carry out, especially when installed on building facades.

The problem of faulty antennas has been extensively studied in the field of phased arrays, which share several similarities with RISs. Identification of faulty elements is mainly achieved via compressed sensing [7], [8] in which external probes collect radiation patterns in the near-field and identify the abnormalities in post-processing. In [9], the authors compute the excitation weights for a faulty planar array in order to recover the original array pattern, while other mitigation techniques imply the use of specific hardware and/or active devices [10]. However, in the case of RISs, such methods cannot be applied since purely passive RIS elements cannot amplify impinging signals, and they cannot prevent failing elements from reflecting signals like active transceivers can.

Conversely, the literature investigating faulty RISs is relatively scarce and focuses mainly on the RIS diagnostics point of view, i.e., detecting which elements are faulty and their associated state in terms of signal attenuation and phase shift. The authors of [11] propose methods that, even with limited or absent Channel State Information (CSI), can pinpoint the antenna elements that are behaving irregularly. In [12], two different diagnosis strategies are developed to determine faulty elements and consequently perform user localization. Similarly, the authors of [13] propose an algorithm for faulty element diagnosis via compressed sensing. In [14], the authors formulate an equivalent channel estimation problem and detect the state of faulty RIS elements by specific pilot transmissions.

In this paper, we consider a RIS-aided wireless network where a subset of the available RIS elements experiences failures. Moreover, *unlike existing works that only deal with the detection of faulty RIS elements via advanced channel estimation techniques [11]–[14], we study the problem of mitigating the associated negative effects on the system performance.* Specifically, we point out that, even in cases when faulty RIS elements do not degrade the Signal-to-Noise-Ratio (SNR) at the intended User Equipment (UE) significantly, the information signal is spread along unwanted directions causing a sharp increase in *signal leakage* to unintended UEs (causing interference) or potential eavesdroppers.

This work was supported by EU FP for Research and Innovation Horizon 2020 under Grant Agreements No. 861222 (MINTS), No. 101017011 (RISE-6G), and No. 101017109 (DAEMON) projects.

To address this problem, we develop a mathematical approach for optimizing the RIS configuration that maximizes the Signal-to-Leakage-and-Noise-Ratio (SLNR) by exploiting only geometrical information on the two-dimensional (2D) area wherein the intended UE is located, thus effectively overcoming the negative impact of the faulty elements. To the best of our knowledge, our approach is the first to consider the SLNR as optimization metric in RIS-aided networks, and is applicable both for the case of perfect CSI, i.e., when the position and state of the faulty elements is known, and in the case of partial CSI, i.e., when the state of the faulty elements is unknown. We provide numerical results demonstrating remarkable benefits with our proposed approaches of up to 35% and 20% improvement in SLNR under perfect and partial CSI, respectively, as compared to *agnostic* schemes that ignore the presence of faulty elements, and *naive* approaches that *simply* aim at maximizing SNR, thus ignoring the signal leakage. Such gains are achieved at a small cost of less than 4% in terms of SNR.

Notation. Matrices and vectors are denoted in uppercase and lowercase bold font, respectively. $(\cdot)^{\mathrm{T}}$, $(\cdot)^{\mathrm{H}}$, and $\mathrm{tr}(\cdot)$ stand for transposition, Hermitian transposition, and trace of a square matrix, respectively. $\|\cdot\|$ denotes the Euclidean norm, while $|\cdot|$ and $\angle\cdot$ denote the absolute value and phase of a complex number, respectively. Lastly, $j = \sqrt{-1}$ is the imaginary number, and $\mathrm{diag}(\mathbf{x})$ is a square matrix whose diagonal is equal to $\mathbf{x}$ and all other elements are zero.

II. System Model

We consider a downlink Multiple Input, Single Output (MISO) wireless network,[1] wherein an Access Point (AP) equipped with M antennas, a RIS equipped with N antennas in Line-of-Sight (LOS) with the AP, and an intended UE are deployed, as depicted in Fig. 1. Furthermore, we assume that the direct link between the AP and the UE is blocked, i.e., in Non-Line-of-Sight (NLOS). Let $\mathbf{h}_k \in \mathbb{C}^{N\times 1}$ and $\mathbf{G} \in \mathbb{C}^{N\times M}$ denote the channel from the RIS to UE k and from the AP to the RIS, respectively. Hence, the receive signal at the intended UE k is given by

$$y_k = \mathbf{h}_k^{\mathrm{H}}\mathbf{\Phi}\mathbf{G}\mathbf{w}_k s + n \in \mathbb{C}, \tag{1}$$

where $\mathbf{\Phi} = \mathrm{diag}[e^{j\theta_1}, \dots, e^{j\theta_N}] \in \mathbb{C}^{N\times N}$ denotes the matrix of RIS phase shifts, $\mathbf{w}_k = \sqrt{P}\frac{\mathbf{G}^{\mathrm{H}}\mathbf{\Phi}^{\mathrm{H}}\mathbf{h}_k}{\|\mathbf{G}^{\mathrm{H}}\mathbf{\Phi}^{\mathrm{H}}\mathbf{h}_k\|} \in \mathbb{C}^{M\times 1}$ is the maximum-ratio transmission (MRT) precoder that maximizes the SNR for the effective channel between the AP and the UE through the RIS, with P the power budget, $s \in \mathbb{C}$ is the transmit symbol, with $\mathbb{E}[|s|^2] = 1$, and $n \in \mathbb{C}$ is the noise coefficient distributed as $\mathcal{CN}(0, \sigma_n^2)$. For simplicity, we rewrite the received signal in (1) as

$$y_k = \mathbf{v}^{\mathrm{H}}\bar{\mathbf{H}}_k\mathbf{w}_k s + n, \tag{2}$$

$$= \sqrt{P}\|\mathbf{v}^{\mathrm{H}}\bar{\mathbf{H}}_k\|s + n \tag{3}$$

where $\mathbf{v} = \mathrm{diag}(\mathbf{\Phi}^{\mathrm{H}}) \in \mathbb{C}^{N\times 1}$, $\bar{\mathbf{H}}_k = \mathrm{diag}(\mathbf{h}_k^{\mathrm{H}})\mathbf{G} \in \mathbb{C}^{N\times M}$, and we have used the expression of the precoder.

[1]Note that, in order to simplify the presentation, we focus on a MISO system. However, the extension to a Multiple Input, Multiple Output (MIMO) setting is readily obtained by simply implementing receive combining.

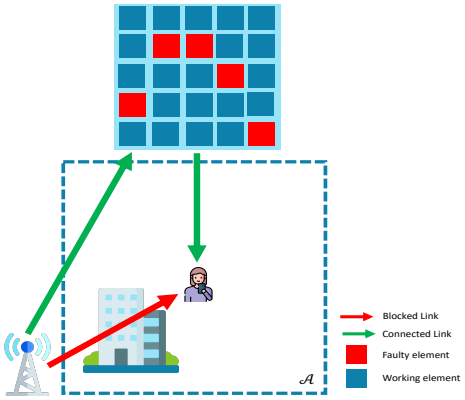

Fig. 1: System model.

A. Baseline model

We define the SNR at the intended UE location as

$$\mathrm{SNR} = \frac{P\,\|\mathbf{v}^{\mathrm{H}}\bar{\mathbf{H}}_k\|^2}{\sigma_n^2}. \tag{4}$$

Hence, the objective of the baseline scheme is formalized as

$$\begin{aligned} \max_{\mathbf{v}} \quad & \mathrm{SNR} \\ \text{s.t.} \quad & |v_n| = 1, \quad n = 1, \dots, N, \end{aligned} \tag{5}$$

whose closed-form solution is given by

$$\mathbf{v}_{BL} = e^{j\angle\bar{\mathbf{h}}_{k,1}} \in \mathbb{C}^{N\times 1}, \tag{6}$$

where the subscript BL stands for *baseline*, $\bar{\mathbf{h}}_{k,1}$ is the eigenvector associated to the only non-zero eigenvalue of $\bar{\mathbf{H}}_k$, which is a rank-1 matrix due to the LOS channel between the AP and the RIS.

B. Faulty RIS model

We assume that a total of $B \leq N$ RIS elements are faulty, such that $\mathbf{v} = [\mathbf{v}_{\mathrm{R}}^{\mathrm{T}}\ \mathbf{v}_{\mathrm{B}}^{\mathrm{T}}]^{\mathrm{T}}$ and $\bar{\mathbf{H}}_k = [\bar{\mathbf{H}}_{\mathrm{R},k}^{\mathrm{T}}\ \bar{\mathbf{H}}_{\mathrm{B},k}^{\mathrm{T}}]^{\mathrm{T}}$, where each $v_{\mathrm{B},b},\ b = 1, \dots, B$ is a Random Variable (RV) with $|v_{\mathrm{B},b}| \leq 1$, $B \leq N$, and $\angle v_{\mathrm{B},b} \in [0, 2\pi)$, $\bar{\mathbf{H}}_{\mathrm{R},k} \in \mathbb{C}^{N-B\times M}$ and $\bar{\mathbf{H}}_{\mathrm{B},k} \in \mathbb{C}^{B\times M}$. In this regard, the subvector $\mathbf{v}_{\mathrm{R}} \in \mathbb{C}^{N-B\times 1}$ represents the tunable RIS elements that are fully functioning, whereas $\mathbf{v}_{\mathrm{B}} \in \mathbb{C}^{B\times 1}$ denotes the uncontrollable faulty elements. We thus rewrite the receive signal in (2) as

$$y_k = \begin{bmatrix}\mathbf{v}_{\mathrm{R}}^{\mathrm{H}} & \mathbf{v}_{\mathrm{B}}^{\mathrm{H}}\end{bmatrix}\begin{bmatrix}\bar{\mathbf{H}}_{\mathrm{R},k} \\ \bar{\mathbf{H}}_{\mathrm{B},k}\end{bmatrix}\mathbf{w}_k s + n \tag{7}$$

$$= (\mathbf{v}_{\mathrm{R}}^{\mathrm{H}}\bar{\mathbf{H}}_{\mathrm{R},k} + \mathbf{h}_{\mathrm{B},k}^{\mathrm{H}})\mathbf{w}_k s + n, \tag{8}$$

where we have defined

$$\mathbf{h}_{\mathrm{B},k}^{\mathrm{H}} = \mathbf{v}_{\mathrm{B}}^{\mathrm{H}}\bar{\mathbf{H}}_{\mathrm{B},k} \in \mathbb{C}^{1\times M}, \tag{9}$$

which is treated as a fixed channel component, since it is uncontrollable by the RIS. Note that with this simple modelling, the received signal in (8) is in the form of an equivalent LOS MISO RIS-aided network [15]. The SNR is thus re-written as

$$\mathrm{SNR} = \frac{P\,\|\mathbf{v}_{\mathrm{R}}^{\mathrm{H}}\bar{\mathbf{H}}_{\mathrm{R},k} + \mathbf{h}_{\mathrm{B},k}^{\mathrm{H}}\|^2}{\sigma_n^2}. \tag{10}$$

III. Problem formulation and solution

In this section, we analyze potential mitigation strategies under the assumption of perfect or partial CSI information at the AP, i.e., the exact values of $\mathbf{v}_{\mathrm{B}}$, or only the indexes of the faulty elements, respectively.

A. Maximum SNR

As a first simple mitigation technique, we analyze the problem of maximizing the SNR at the intended UE. Given the equivalent model in (8) and (10), let us define

$$\mathbf{V}_{\mathrm{R}} = \begin{bmatrix} \mathbf{v}_{\mathrm{R}} \\ 1 \end{bmatrix} \begin{bmatrix} \mathbf{v}_{\mathrm{R}}^{\mathrm{H}} & 1 \end{bmatrix} \in \mathbb{C}^{\bar{N}+1 \times \bar{N}+1}, b \tag{11}$$

where $\bar{N} = N - B$ is the number of functioning RIS elements. Hence, the RIS configuration that maximizes the SNR under RIS element failures is given by

Problem 1:

$$\begin{aligned} \max_{\mathbf{V}_{\mathrm{R}} \succeq \mathbf{0}} \quad & \mathrm{tr}(\mathbf{V}_{\mathrm{R}} \widetilde{\mathbf{H}}_k) \\ \text{s.t.} \quad & \mathrm{diag}(\mathbf{V}_{\mathrm{R}}) = \mathbf{1}, \quad \mathrm{rank}(\mathbf{V}_{\mathrm{R}}) = 1, \end{aligned} \tag{12}$$

where we have defined

$$\widetilde{\mathbf{H}}_k = \begin{bmatrix} \bar{\mathbf{H}}_{\mathrm{R},k} \\ \mathbf{h}_{\mathrm{B},k}^{\mathrm{H}} \end{bmatrix} \begin{bmatrix} \bar{\mathbf{H}}_{\mathrm{R},k}^{\mathrm{H}} & \mathbf{h}_{\mathrm{B},k} \end{bmatrix} \in \mathbb{C}^{\bar{N}+1 \times \bar{N}+1}. \tag{13}$$

Problem 1 can be solved by semi-definite relaxation (SDR), i.e., ignoring the rank-one constraint and then approximating the RIS configuration $\mathbf{v}_{\mathrm{R}}$ via randomization techniques [16]. Note that the RIS configuration obtained as a result of the aforementioned procedure aims at aligning the signal bouncing off the *functioning* RIS elements with the (random) channel component that is in the direction of the UE and originated from the superposition of the signal reflected by the *faulty* RIS elements. We denote this method as *naive* RIS optimization.

B. Maximum SLNR

In this case, our aim is not only to improve the SNR at the intended receiver by compensating for the effect of the faulty RIS elements, but to jointly minimize potential leakage to non-intended UEs or eavesdroppers in the proximity of the UE as well. Moreover, our proposed approach exploits geometrical information only, without the need of acquiring costly CSI of potentially non-intended UEs. In this regard, we assume that all UEs are located within a three-dimensional area $\mathcal{A}$. Let $\mathbf{p} \in \mathcal{A} \subset \mathbb{R}^3$ be the location of a potential non-intended UE, such that the *leakage* over such area is given by

$$\mathrm{L}(\mathcal{A}) = \int_{\mathcal{A}} \|\mathbf{v}_{\mathrm{R}}^{\mathrm{H}} \bar{\mathbf{H}}_{\mathrm{R}}(\mathbf{p}) + \mathbf{h}_{\mathrm{B}}^{\mathrm{H}}(\mathbf{p})\|^2 \mathrm{d}\mathbf{p}, \tag{14}$$

where $\bar{\mathbf{H}}_{\mathrm{R}}(\mathbf{p}) \in \mathbb{C}^{N \times M}$ is the equivalent channel from the AP to the point $\mathbf{p}$, through the functioning RIS elements, and $\mathbf{h}_{\mathrm{B}}^{\mathrm{H}}(\mathbf{p}) \in \mathbb{C}^{1 \times M}$ is the equivalent direct and uncontrollable channel between the AP and position $\mathbf{p}$, through the faulty RIS elements. Therefore, we define the SLNR as

$$\mathrm{SLNR} = \frac{\|(\mathbf{v}_{\mathrm{R}}^{\mathrm{H}} \bar{\mathbf{H}}_{\mathrm{R},k} + \mathbf{h}_{\mathrm{B},k}^{\mathrm{H}})\|^2}{\mathrm{L}(\mathcal{A}) + \sigma_n^2/P}. \tag{15}$$

Given the complex structure of (15), we discretize the area $\mathcal{A}$ into T *test points* such that the SLNR is approximated as

$$\mathrm{SLNR} \approx \frac{\|(\mathbf{v}_{\mathrm{R}}^{\mathrm{H}} \bar{\mathbf{H}}_{\mathrm{R},k} + \mathbf{h}_{\mathrm{B},k}^{\mathrm{H}})\|^2}{\sum_{t=1, t \neq k}^{T} \|(\mathbf{v}_{\mathrm{R}}^{\mathrm{H}} \bar{\mathbf{H}}_{\mathrm{R},t} + \mathbf{h}_{\mathrm{B},t}^{\mathrm{H}})\|^2 + \sigma_n^2/P}, \tag{16}$$

which is a sampled version of (15). However, the objective function in (16) might be maximized by focusing on minimizing the denominator, i.e., the leakage, at the cost of a reduction in the numerator, i.e., the useful signal power. Hence, to avoid obtaining a trivial solution, we add a minimum SNR requirement, which is necessary to decode the signal, and formulate the following optimization problem

Problem 2:

$$\begin{aligned} \max_{\mathbf{v}_{\mathrm{R}}} \quad & \mathrm{SLNR} \\ \text{s.t.} \quad & \|(\mathbf{v}_{\mathrm{R}}^{\mathrm{H}} \bar{\mathbf{H}}_{\mathrm{R},k} + \mathbf{h}_{\mathrm{B},k}^{\mathrm{H}})\|^2 \geq \gamma \\ & |v_{\mathrm{R},n}| = 1, \quad n = 1, \ldots, \bar{N}, \end{aligned} \tag{17}$$

where the system parameter γ regulates the trade-off between leakage reduction and useful signal power.

By using the definition in (11), we have that

$$\begin{aligned} \|(\mathbf{v}_{\mathrm{R}}^{\mathrm{H}} \bar{\mathbf{H}}_{\mathrm{R},k} + \mathbf{h}_{\mathrm{B},k}^{\mathrm{H}})\|^2 &= \left\| \begin{bmatrix} \mathbf{v}_{\mathrm{R}}^{\mathrm{H}} & 1 \end{bmatrix} \begin{bmatrix} \bar{\mathbf{H}}_{\mathrm{R},k} \\ \mathbf{h}_{\mathrm{B},k}^{\mathrm{H}} \end{bmatrix} \right\|^2 \\ &= \mathrm{tr}(\widetilde{\mathbf{H}}_k \mathbf{V}_{\mathrm{R}}), \end{aligned} \tag{18}$$

where $\widetilde{\mathbf{H}}_k$ is defined in (13).

By making use of the bisection method, we can rewrite Problem 2 as [17]

Problem 3:

$$\begin{aligned} \max_{\beta \geq 0, \mathbf{V}_{\mathrm{R}} \succeq \mathbf{0}} \quad & \beta \\ \text{s.t.} \quad & \mathrm{tr}(\widetilde{\mathbf{H}}_k \mathbf{V}_{\mathrm{R}}) \geq \beta \left(\sum_{t=1, t \neq k}^{T} \mathrm{tr}(\widetilde{\mathbf{H}}_t \mathbf{V}_{\mathrm{R}}) + \sigma_n^2/P \right) \\ & \mathrm{tr}(\widetilde{\mathbf{H}}_k \mathbf{V}_{\mathrm{R}}) \geq \gamma \\ & \mathrm{diag}(\mathbf{V}_{\mathrm{R}}) = \mathbf{1}, \ \mathrm{rank}(\mathbf{V}_{\mathrm{R}}) = 1. \end{aligned} \tag{19}$$

Problem 3 is solved via SDR, i.e., by ignoring the non-convex rank constraint and then extracting a rank-1 solution via randomization techniques [16]. The resulting algorithm is formalized in Algorithm 1.

C. Partial CSI case: robust solution

In the following, we describe a faulty RIS mitigation strategy, which relaxes the assumption of perfect CSI and considers only knowledge of the position of the faulty elements, and not their actual phase-shifting value. In this regard, we consider the maximization of the average SLNR, where the average is taken over the random realizations of the phase shift and amplitude attenuation applied at the faulty elements. However, since the SLNR in (16) is a fractional function, for the sake of simplicity, and given the independence among the numerator and denominator, we employ Jensen's inequality and optimize a lower bound on the expected SLNR as

$$\mathbb{E}[\mathrm{SLNR}] \geq \frac{\mathbb{E}[\|(\mathbf{v}_{\mathrm{R}}^{\mathrm{H}} \bar{\mathbf{H}}_{\mathrm{R},k} + \mathbf{h}_{\mathrm{B},k}^{\mathrm{H}})\|^2]}{\sum_{t=1, t \neq k}^{T} \mathbb{E}[\|(\mathbf{v}_{\mathrm{R}}^{\mathrm{H}} \bar{\mathbf{H}}_{\mathrm{R},t} + \mathbf{h}_{\mathrm{B},t}^{\mathrm{H}})\|^2] + \sigma_n^2/P}. \tag{20}$$

Algorithm 1: Iterative algorithm for Problem 3

Initialize $h^{(0)}$, $l^{(0)}$, δ, and γ to feasible values
repeat *Bisection loop (over i)*
  Set $\beta = \frac{h^{(i)}+l^{(i)}}{2}$
  if *Problem 3 admits a a feasible solution $\mathbf{V}_{\mathrm{R}}^{\star}$ by using SDR* **then**
    Set $l^{(i+1)} = \beta$ and $h^{(i+1)} = h^{(i)}$
  else
    Set $h^{(i+1)} = \beta$ and $l^{(i+1)} = l^{(i)}$
  end
until $|h^{(i)} - l^{(i)}|/|h^{(i)}| < \delta$
Extract $\mathbf{v}_{\mathrm{R}}^{\star}$ from $\mathbf{V}_{\mathrm{R}}^{\star}$ via Gaussian randomization

As explained in Section II-B, we model the effect caused by the faulty elements as $v_{\mathrm{B},i} = \delta_i e^{j\phi_i}$ where $\delta_i \sim \mathcal{U}[0,1]$ and $\phi_i \sim \mathcal{U}[0, 2\pi)$. Hence, we have that

$$\mathbb{E}[\|(\mathbf{v}_{\mathrm{R}}^{\mathrm{H}}\bar{\mathbf{H}}_{\mathrm{R},k} + \mathbf{h}_{\mathrm{B},k}^{\mathrm{H}})\|^2] = \|\mathbf{v}_{\mathrm{R}}^{\mathrm{H}}\bar{\mathbf{H}}_{\mathrm{R},k}\|^2 + \mathbb{E}[\|\mathbf{v}_{\mathrm{B}}^{\mathrm{H}}\bar{\mathbf{H}}_{\mathrm{B},k}\|^2] + 2\,\mathrm{Re}\{\mathbf{v}_{\mathrm{R}}^{\mathrm{H}}\bar{\mathbf{H}}_{\mathrm{R},k}\bar{\mathbf{H}}_{\mathrm{B},k}^{\mathrm{H}}\mathbb{E}[\mathbf{v}_{\mathrm{B}}]\}. \quad (21)$$

We now examine $\mathbb{E}[\mathbf{v}_{\mathrm{B}}]$ as

$$\begin{aligned}\mathbb{E}[v_{\mathrm{B},i}] &= \mathbb{E}[\delta_i e^{j\phi_i}] \quad (22)\\ &= \mathbb{E}[\delta_i](\mathbb{E}[\cos(\phi_i)] + j\mathbb{E}[\sin(\phi_i)])\\ &= 0 \quad \forall i,\end{aligned}$$

which leads to

$$\mathbb{E}[\|\mathbf{v}_{\mathrm{B}}^{\mathrm{H}}\bar{\mathbf{H}}_{\mathrm{B},k}\|^2] = \sum_i \mathbb{E}[|\mathbf{v}_{\mathrm{B}}^{\mathrm{H}}\bar{\mathbf{h}}_{\mathrm{B},k,i}|^2] \quad (23)$$

$$= \sum_i \mathbb{E}\left[\left|\sum_j v_{\mathrm{B},j}^{*}\bar{H}_{\mathrm{B},k,i,j}\right|^2\right], \quad (24)$$

where $\bar{\mathbf{h}}_{\mathrm{B},k,i}$ is the i-th column of $\bar{\mathbf{H}}_{\mathrm{B},k}$. The expression in (24) leads to $\mathbb{E}[\|\mathbf{v}_{\mathrm{B}}^{\mathrm{H}}\bar{\mathbf{H}}_{\mathrm{B},k}\|^2] = \frac{1}{3}\|\bar{\mathbf{H}}_{\mathrm{B},k}\|_{\mathrm{F}}^2$ given the independence among the states of the faulty RIS elements and the fact that $\mathbb{E}[\delta_i^2] = 1/3$. Similarly, we obtain $\mathbb{E}[\|\mathbf{v}_{\mathrm{B}}^{\mathrm{H}}\bar{\mathbf{H}}_{\mathrm{B},t}\|^2] = \frac{1}{3}\|\bar{\mathbf{H}}_{\mathrm{B},t}\|_{\mathrm{F}}^2, \quad \forall t$. The lower bound on the expected SLNR is thus rewritten as

$$\mathbb{E}[\mathrm{SLNR}] \geq \frac{\|\mathbf{v}_{\mathrm{R}}^{\mathrm{H}}\bar{\mathbf{H}}_{\mathrm{R},k}\|^2 + \frac{1}{3}\|\bar{\mathbf{H}}_{\mathrm{B},k}\|_{\mathrm{F}}^2}{\sum_{t=1,t\neq k}^{T}\|\mathbf{v}_{\mathrm{R}}^{\mathrm{H}}\bar{\mathbf{H}}_{\mathrm{R},t}\|^2 + \frac{1}{3}\|\bar{\mathbf{H}}_{\mathrm{B},t}\|_{\mathrm{F}}^2 + \sigma_n^2/P}. \quad (25)$$

Therefore, we obtain a robust mitigation solution for faulty RISs by applying Algorithm 1 with $\mathbf{h}_{\mathrm{B},k} = \mathbf{h}_{\mathrm{B},t} = \mathbf{0}, \quad \forall t$ and by adding the constant offsets $\frac{1}{3}\|\bar{\mathbf{H}}_{\mathrm{B},k}\|_{\mathrm{F}}^2$ and $\sum_{t=1,t\neq k}^{T}\frac{1}{3}\|\bar{\mathbf{H}}_{\mathrm{B},t}\|_{\mathrm{F}}^2$ to the LHS and the RHS of the first constrain in Problem (3), respectively.

IV. Numerical results and discussion

In this section, we assess the performance of our proposed frameworks targeting the maximization of the instantaneous and average SLNR, against the reference schemes, namely the leakage-unaware *baseline* and the *naive* approach targeting the maximization of the SNR, by evaluating both the obtained SLNR and SNR in realistic settings.

A. Channel model

We consider a Rician channel model for the RIS-UE link, and a LOS channel for the AP-RIS link The channel between the RIS and the UE is given by [15]

$$\mathbf{h}_k \triangleq \sqrt{\frac{K_{\mathrm{R}}}{1+K_{\mathrm{R}}}}\,\mathbf{h}_k^{\mathrm{LoS}} + \sqrt{\frac{1}{1+K_{\mathrm{R}}}}\,\mathbf{h}_k^{\mathrm{NLoS}} \in \mathbb{C}^{N\times 1}, \quad (26)$$

where K_{R} is the Rician factor. Moreover, the LOS link from the RIS to the UE is defined as

$$\mathbf{h}_k^{\mathrm{LoS}} \triangleq \sqrt{\gamma_g}\,\mathbf{b}(\psi_k) \in \mathbb{C}^{N\times 1}, \quad (27)$$

where the distance-dependent pathloss is represented as $\gamma_g = \zeta_0/(d_2)^{\eta_r}$, with ζ_0, d_2, and η_r being the free-space loss factor at a reference distance of one meter [18], the distance between the RIS and the UE, and the corresponding pathloss exponent, respectively. $\mathbf{b}(\psi_k)$ is the array steering vector for the Angle of Departure (AoD) ψ_k defined as

$$\mathbf{b}(\psi_k) = [1, e^{j\frac{2\pi}{\lambda}d\cos(\psi_k)}, \ldots, e^{j(N-1)\frac{2\pi}{\lambda}d\cos(\psi_k)}]^{\mathrm{T}} \in \mathbb{C}^{N\times 1}, \quad (28)$$

where λ represents the signal wavelength, and $d = \lambda/2$ the inter-element spacing. Note that the LOS AP-RIS link $\mathbf{G}$ is obtained in a similar manner as

$$\mathbf{G} \triangleq \sqrt{\gamma_i}\,\mathbf{b}(\psi_A)\mathbf{a}(\psi_D)^{\mathrm{H}} \in \mathbb{C}^{N\times M}, \quad (29)$$

where ψ_A, ψ_D are the Angle of Arrival (AoA) and AoD, respectively, while $\mathbf{a}(\psi_D) \in \mathbb{C}^{M\times 1}$ is the steering vector at the AP, and $\gamma_i = \zeta_0/(d_1)^{\eta_i}$ is the distance-dependent pathloss for the AP-RIS link, with d_1 and η_i the distance between the AP and the RIS, and its associated pathloss exponent, respectively. Lastly, the NLOS link from the RIS to the UE is defined as

$$\mathbf{h}_k^{\mathrm{NLoS}} \triangleq \sqrt{\frac{\gamma_g}{P_K}}\sum_{p=1}^{P_K}\mathbf{G}_p^{(w)} \circ \mathbf{b}(\psi_{A,p}) \in \mathbb{C}^{N\times 1}, \quad (30)$$

where P_K represents the total number of scattering paths, $\mathbf{G}_p^{(w)}$ is the small scale fading coefficient of the p-th path with $\mathrm{vec}(\mathbf{G}_p^{(w)}) \sim \mathcal{CN}(\mathbf{0}, \mathbf{I}_N)$, $\circ$ denotes the Hadamard product, and $\psi_{A,p}$ is the AoD of the p-th path.

B. Simulation setup

We consider a wireless network wherein an AP equipped with a 16-antenna Uniform Linear Array (ULA) is assisted by a RIS with $N = N_x N_y$ elements where $N_x = 10$ elements are placed on the x-axis, and $N_y = 10$ elements are placed on the y-axis. We assume that the UE, RIS, and the AP are located at the three-dimensional coordinates of $\mathbf{p}_{\mathrm{UE}} = (16, 16, 0)$, $\mathbf{p}_{\mathrm{RIS}} = (10, 34, 10)$, and $\mathbf{p}_{\mathrm{AP}} = (0, 0, 10)$, respectively. The AP is assumed to be transmitting at the carrier frequency of 30 GHz with a power of $P = 12$ dBm per subcarrier while the noise power is assumed to be $\sigma_n^2 = -80$ dBm. For the RIS-UE link, we account for $P_K = 10$ different scattering paths, and we set the Rician factor to $K_R = 10$ dB and the pathloss exponent as $\eta_r = 2$. The threshold SNR value γ in Algorithm 1 is set by dividing the SNR of the naive approach by 1.5. The intended UE is located at the center of a target area $\mathcal{A}$ of dimension 30×30 m. We sample such

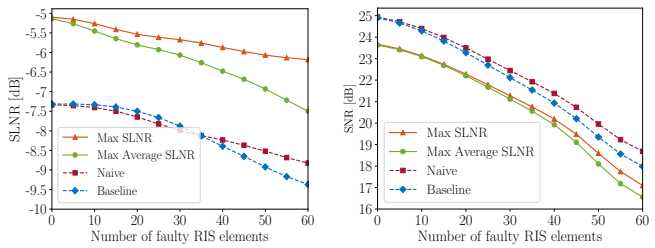

(a) Achievable SLNR (b) Cost paid in terms of SNR.

Fig. 2: Comparison in terms of SLNR and SNR between the proposed approaches under perfect and partial CSI, and the reference schemes, versus the number of faulty RIS elements.

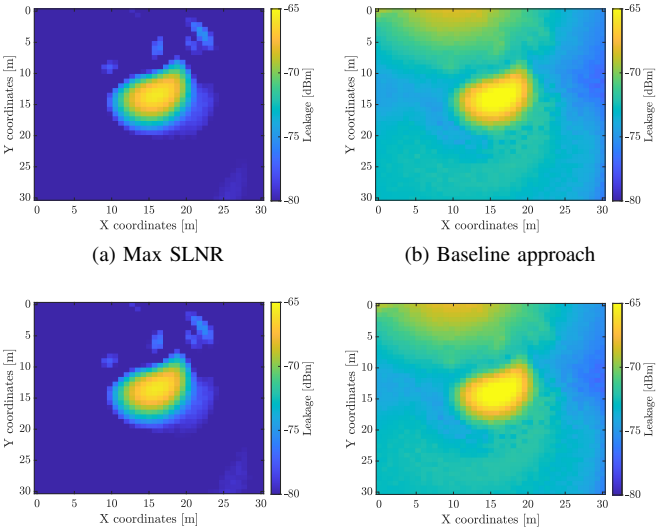

(a) Max SLNR (b) Baseline approach

(c) Max Average SLNR (d) Naive approach

Fig. 3: Heatmap of the received power in dBm over the target area with 10% faulty RIS elements for the proposed approaches, i.e., (a) SLNR maximization under perfect CSI and (c) SLNR maximization under partial CSI, and the reference schemes, i.e., (b) baseline approach and (d) naive approach.

area in a set of $T = 125$ uniformly scattered *leakage points*. Moreover, we assume that the RIS elements fail according to a uniform distribution, unless otherwise stated, and we average our results over 10^3 independent realizations of the faulty RIS elements position and state, as well as the location of the leakage points. All relevant simulation parameters are summarized in Table I.

TABLE I: Simulation parameters.

Parameter	Value	Parameter	Value	Parameter	Value
N	100	λ	10 mm	σ_n^2	-80 dBm
P	12 dBm	K_{R}	10 dB	P_K	10
η_i	2	η_r	2	$\mathbf{p}_{\mathrm{AP}}$	$(0, 0, 10)$
$\mathbf{p}_{\mathrm{RIS}}$	$(10, 34, 10)$	$\mathbf{p}_{\mathrm{UE}}$	$(16, 16, 0)$	T	125

C. Discussion

In Fig. 2a, we compare the performance of the proposed approaches under perfect and partial CSI, denoted as *Max SLNR* and *Max Average SLNR*, respectively, along with the baseline and naive approaches, in terms of the achievable

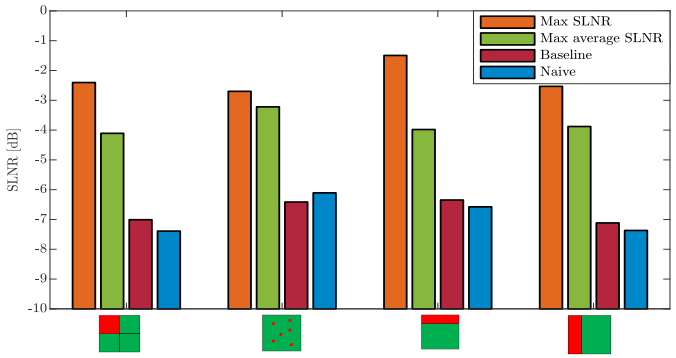

Fig. 4: SLNR obtained with the proposed approaches and the reference schemes versus different distributions of 25% of faulty antenna elements at the RIS (marked in red).

SLNR versus the number of faulty RIS elements. For increasing number of faulty RIS elements, the SLNR tends to decrease rapidly. However, the proposed approaches obtain significantly higher performance and resilience to faulty RISs, especially in the case of perfect CSI at the cost of a small reduction in SNR, as shown in Fig. 2b. Here, as expected, the naive approach obtains the highest value, though neglecting signal leakage. To better understand the effectiveness of our proposed approaches, in Fig. 3 we show the 2D heatmap of the received power over the target area wherein the intended UE is located, i.e., the signal leakage, for the case of 10 faulty RIS elements. Fig. 3a and Fig. 3c show considerable improvement in terms of the signal leakage received in the target area as compared to the reference schemes in Fig. 3b and Fig. 3d. Indeed, for the proposed schemes the signal power is high only in the close-proximity of the UE, whereas for the reference schemes the average received power is significantly higher elsewhere, especially close to the RIS (i.e., the upper-left corner of the figures).

Lastly, in Fig. 4 we evaluate the impact of the distribution of 25% of faulty RIS elements on the SLNR. We consider four cases, namely *i)* the upper-left quadrant of the RIS fails, *ii)* uniform distribution of the faulty RIS elements (as is the case for the rest of the figures), *iii)* the upper two rows of the RIS fail, and *iv)* the first two columns starting from the left of the RIS fail. In all considered scenarios, the proposed schemes outperform the reference schemes. In particular, we infer that having the faulty elements grouped together represents a worst-case scenario for the reference schemes, since this originates strong side lobes pointing towards fixed directions. Conversely, the opposite is true for the proposed schemes: in the case of partial CSI, the performance is equivalent in all cases, while in the case of perfect CSI the proposed approach manages to mitigate the unwanted signal spreading especially when the distribution of the faulty elements is not uniform.

D. Full-wave simulations

In this section, we demonstrate the effectiveness of our proposed approach in the case of perfect CSI versus the baseline scheme for the case of 10% faulty RIS elements using a full-wave simulator, CST Studio Suite 2019. Fig. 5 shows the far-field radiation pattern as the spherical coordinates *Theta*

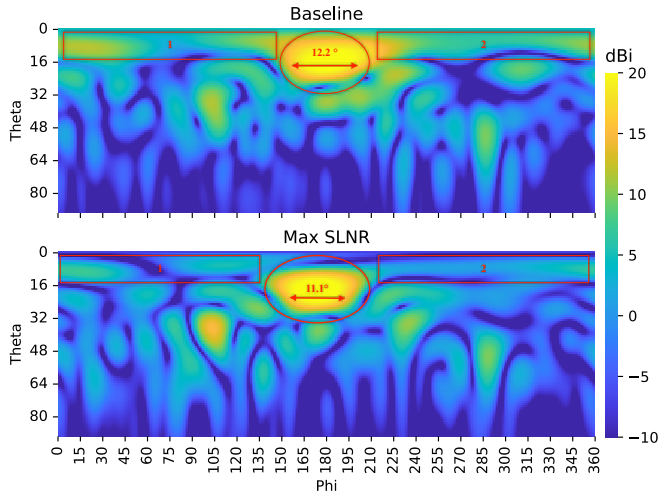

Fig. 5: Full-wave simulation of the far-field radiation pattern obtained with the proposed approach for perfect CSI and the baseline.

and *Phi* vary along the azimuth and elevation directions, respectively. In the range of $[0°, 15°]$ in azimuth, the baseline approach exhibits an average power of 16.8 and 16.3 dBi, which are marked with two red boxes, respectively, and a main beam with a half power beamwidth of 12.2°. On the contrary, the proposed approach manages to significantly reduce the power outside the main beam pointing towards the UE (average of 11.2 and 9.8 dBi, respectively), with its half power beamwidth reduced to 11.1°. Hence, the proposed approach mitigates the undesired side lobes while better focusing the power towards a specific direction. Indeed, when there are faulty elements on the RIS, the behavior of the RIS becomes similar to an omnidirectional antenna, thus reflecting the signal to all directions. This effect can be clearly seen in Fig. 6, which shows the full-wave simulation of the 3D beampattern for the considered schemes. As expected, the proposed approach exhibits a narrower main beam and lower side lobes as compared to the baseline scheme.

V. Conclusions

In this paper, we have proposed a novel mathematical framework to address the problem of mitigating unintentional signal leakage caused by faulty RIS elements, which may result in additional interference to non-intended UEs and security threats to potential eavesdroppers. Specifically, we have formulated a low-complexity model for the random signal attenuation and phase shift introduced by each faulty RIS element, and we have proposed a proven convergent iterative algorithm that targets the optimization of the functioning RIS elements by maximizing the SLNR in a given 2D area wherein the intended UE is located. This approach is applicable in the case of both perfect CSI, i.e., when the location and state of the faulty elements are known, and in the case of partial CSI, i.e., when the state of the faulty elements is unknown. Numerical results have demonstrated the effectiveness of the proposed approaches in terms of achievable SLNR (up to 35% improvement), at the cost of a small reduction in SNR (within 4%) as compared to other reference schemes.

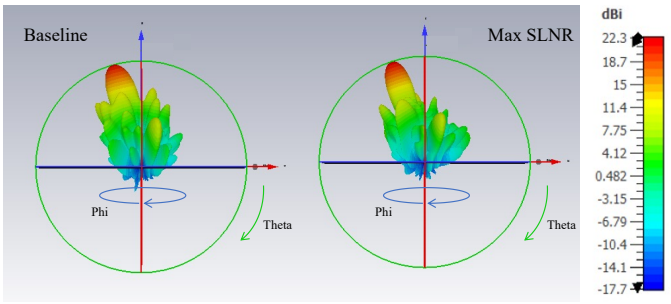

Fig. 6: Full-wave simulation of the 3D beampattern obtained with the proposed approach for perfect CSI and the baseline.

Several intriguing research directions, involve the exploration of network challenges in cases of multiple RISs or multiple UEs, and refining optimization problems related to these contexts.

References

[1] M. di Renzo, M. Debbah *et al.*, "Smart radio environments empowered by ai reconfigurable meta-surfaces: An idea whose time has come," *EURASIP J. on Wireless Commun and Netw.*, vol. 129, 2019.

[2] Q. Wu and R. Zhang, "Intelligent reflecting surface enhanced wireless network via joint active and passive beamforming," vol. 18, no. 11, pp. 5394–5409, 2019.

[3] M. Rossanese, P. Mursia *et al.*, "Designing, building, and characterizing rf switch-based reconfigurable intelligent surfaces," in *16th ACM Workshop on Wireless Netw. Testbeds, Experim. eval. & CHaracter. (WiNTECH)*, 2022, p. 69–76.

[4] P. Mursia, S. Phang, *et al.*, "Saris: Scattering aware reconfigurable intelligent surface model and optimization for complex propagation channels," *IEEE Wireless Communications Letters*, 2023.

[5] P. Mursia, F. Devoti *et al.*, "Rise of flight: Ris-empowered uav communications for robust and reliable air-to-ground networks," *IEEE Open J. of the Commun. Soc.*, vol. 2, pp. 1616–1629, 2021.

[6] S. Kisseleff, S. Chatzinotas, and B. Ottersten, "Reconfigurable intelligent surfaces in challenging environments: Underwater, underground, industrial and disaster," *IEEE Access*, vol. 9, pp. 150 214–150 233, 2021.

[7] C. Xiong, G. Xiao *et al.*, "A compressed sensing-based element failure diagnosis method for phased array antenna during beam steering," vol. 18, no. 9, pp. 1756–1760, 2019.

[8] M. E. Eltayeb, T. Y. Al-Naffouri, and R. W. Heath, "Compressive sensing for millimeter wave antenna array diagnosis," vol. 66, no. 6, pp. 2708–2721, 2018.

[9] W. P. Keizer, "Element failure correction for a large monopulse phased array antenna with active amplitude weighting," vol. 55, no. 8, pp. 2211–2218, 2007.

[10] K.-M. Lee, R.-S. Chu, and S.-C. Liu, "A built-in performance-monitoring/fault isolation and correction (pm/fic) system for active phased-array antennas," vol. 41, no. 11, pp. 1530–1540, 1993.

[11] R. Sun, W. Wang *et al.*, "Diagnosis of Intelligent Reflecting Surface in Millimeter-wave Communication Systems," 2021.

[12] C. Ozturk, M. F. Keskin *et al.*, "Ris-aided localization under pixel failures," *arXiv preprint arXiv:2302.04436*, 2023.

[13] S. Ma, J. Li *et al.*, "Joint Diagnosis of RIS and BS for RIS-Aided Millimeter-Wave System," *Electronics*, vol. 10, no. 20, p. 2556, 2021.

[14] B. Li, Z. Zhang *et al.*, "Joint Array Diagnosis and Channel Estimation for RIS-Aided mmWave MIMO System," *IEEE Access*, vol. 8, pp. 193 992–194 006, 2020.

[15] P. Mursia, V. Sciancalepore *et al.*, "RISMA: Reconfigurable Intelligent Surfaces Enabling Beamforming for IoT Massive Access," vol. 39, no. 4, pp. 1072–1085, 2021.

[16] Z. Luo, A. M. So *et al.*, "Semidefinite Relaxation of Quadratic Optimization Problems -From its practical deployments and scope of applicability to key theoretical results-," no. May, pp. 20–34, 2010.

[17] S. Boyd and L. Vandenberghe, *Convex optimization*. Cambridge university press, 2004.

[18] C. A. Balanis, *Antenna Theory: Analysis and Design*, 4th ed. Hoboken, NJ: Wiley, 2016.